1246

Cell Tissue Kinet. (1988), **21**, 247–258.

Intestinal crypt proliferation. II. Computer modelling of mitotic index data provides further evidence for lateral and vertical cell migration in the absence of mitotic activity

M. Loeffler, C.S. Potten*, U. Paulus, J. Glatzer and S. Chwalinski*

*Medizinische Universitätsklinik, Joseph-Stelzmann Strasse 9, D5000 Köln 41, F.R.G. and *Paterson Institute for Cancer Research, Christie Hospital & Holt Radium Institute, Manchester M20 9BX, U.K.*

(*Received* 5 *July* 1987; *revision accepted* 27 *July* 1988)

Abstract. The position-dependent mitotic index before, and 1, 2 and 3 h after vincristine was scored. The accumulation of cells in mitosis leads to an increase in the mitotic index from 0·06 to 0·34 at crypt positions 8–12. Surprisingly, the leading edge of the position-related mitotic index distribution moves to higher crypt positions although cell division was stopped. In addition, the vertical clustering of mitotic figures in sections was recorded. The data were examined using a previously described computer crypt model. We conclude: the average mitotic phase duration is about 0·7 h (40 min) and varies little with cell position; the geometrical correction factor for overscoring mitoses in crypt sections is about 0·6–0·7 and adjacent cell columns can merge. Lateral cell displacement after mitosis, as predicted in a previous model analysis, would be a mechanism to counteract other forces that tend to reduce the crypt circumference. In the normal steady state merging and expansion processes would just balance each other. This would not follow if one mechanism was blocked. Thus we propose a new concept in which the crypt geometry would be dynamically determined by cell proliferative activity in connection with lateral positioning of new cells on one hand and contracting forces on the other hand.

The distribution of the mitotic index (MI) in the murine small intestinal crypts has been examined elsewhere (reviewed in Wright & Alison, 1984; Potten *et al.*, 1982). Nevertheless several points remain unanswered. Firstly, the duration of mitosis is still not precisely known. Measurements have been derived from metaphase arrest data, PLM experiments and from MI distributions which give values between 0·5 and 1·3 h (Wright & Alison, 1984). Secondly, little is known about the positioning of new cells after division. Are they arranged on top of each other or side by side? This question implies an understanding of the migration process in the crypt. Based on a mathematical model analysis of [^{3}H]-thymidine ([^{3}H]TdR) labelling experiments including labelling index (LI) and run distributions, we recently concluded that the percentage

Correspondence: Dr M. Loeffler, Medizinische Universitätsklinik I, Joseph-Stelzmann Strasse 9, D5000 Köln 41, F.R.G.

of lateral displacements after mitosis must be rather high (Loeffler *et al.*, 1986). In this paper we provide further support for this concept which is important because it may have major implications for the understanding of the organization of cell kinetics in the crypt and of the dynamics of the crypt geometry.

Here we analyse in more detail the position-dependent MI distributions and the neighbourhood relationships of mitotic cells in the steady state. We also consider the development of the MI distributions after the stathmokinetic agent vincristine (VCR). We analyse the data with three suitable mathematical models described previously (Loeffler *et al.*, 1986). The first two models (called E and F in that paper) include the basic assumption that the positioning of newborn cells after mitosis is completely determined by the kinetic status (age) of the surrounding (neighbouring) cells. The two models only differ slightly with respect to the number of cells that influence their behaviour. For model E the crypt is strongly age-ordered (younger cells below older cells) with 40 % lateral cell displacements between adjacent cell columns after mitosis. This level of lateral displacement may be an underestimate of the real value; the model F produces a higher number of lateral displacements (65%) but the ordering mechanism is somewhat less effective. In addition, a 'cut-off' model (model H) was considered where the positioning of a new cell in the vicinity of the mother cell was a random process with the transition from the proliferative to the mature stage being determined by external factors related to a particular position in the connective tissue. It was shown that all three models provide acceptable descriptions of the [^{3}H]TdR labelling experiments in steady state situations and we could not discriminate between them.

The analysis of MI data is complicated by the fact that mitotic figures are displaced from the basal membrane of the crypt towards the lumen. This implies that a mitotic figure seen in a section may not originate from the visible cell column but from one out of the section plane. In order to correct for this tendency to overestimate the numbers of mitotic figures, Tannock (1967) suggested the use of a geometrical correction factor which was estimated to be about 0·6. In order to compare exact computer data from full crypts with experimental data from sections a similar factor has to be considered.

METHODS

Experiments

Male BDF_1 mice (about 25 g body weight), 10–12 weeks old, were used. They were housed under standard laboratory conditions with a 12 h light cycle. The small intestine (ileum) was removed intact and fixed in Carnoy's fixative for subsequent embedding in paraffin wax. Several (usually up to 10) segments of ileum were embedded from each mouse according to the procedure described for the crypt micro-colony assay (Potten & Hendry, 1985). In ileal cross sections many good longitudinal sections of individual crypts can be seen and the position of each cell along the side of the crypt (crypt column) in relation to the bottom of the crypt can be easily numerated. Not less than 200 half crypt sections (one side of a longitudinal section through a crypt) were scored (50 from each of the four mice in each group).

The number of mitoses at each position was recorded as described elsewhere (Potten *et al.*, 1982). No correction was made to the data for the coaxial distribution of metaphase figures (Tannock, 1967) since this was assumed to be a constant factor throughout these experiments. Only crypts with a length of at least 17 cell positions were analysed (most were in excess of 20) to avoid the necessity of a crypt length normalization procedure (as suggested by Wright & Alison, 1984). Mitotic figures without any clear contact with the basement membrane which were seen to lie between two cell positions were counted as at an intermediate (half) position. This did not

alter the total number of cells in the crypt column. The MI was calculated as the ratio of all mitotic figures to all the cells seen at a given position (usually 200), or to all the cells in a given zone of the crypt. For the MI, mitotic figures at intermediate positions were scored as a half value for each of the two adjacent positions.

Mathematical models

The mathematical model of the crypt and all the parameters used are described in Loeffler *et al.* (1986). Various alternatives (models A–H) were considered for the positioning of new daughter cells, in particular here we consider the following:

Model A (*only vertical displacement of newborn cells*)

All new daughter cells are arranged on top of each other and the rest of the column then moves one cell position upwards. This model is basically similar to one examined by Meinzer & Sandblad (1985).

Model E (*local age-dependent displacement considering the age or maturity of three neighbouring cells*)

A newly-formed daughter cell selects the oldest of the three immediate neighbour cells to the left, right or above and moves into that position shifting the rest of the selected column one cell position upwards.

Model F (*local age-dependent displacement with five neighbours*)

A newly-formed daughter cell displaces the oldest neighbour to the left, top, right as in model E but also to the top left and top right. The rest of the selected column is then shifted upwards.

Model H (*random displacement of the newborn daughters with a cut-off point determining final maturation*)

One daughter cell is randomly displaced either left, right or upwards. The whole selected column is then shifted upwards. In addition, an environmental influence is imposed determining the final differentiation of transit cells. Cells passing position 12 complete their present cell cycle after which they become post-mitotic cells. All three of the last models (E, F and H) produce good fits to LI and run data (Loeffler *et al.*, 1986).

Simulation and definition of parameters

MI

The MI evaluation in the model resembles the LI evaluation. The MI at position j and time t is defined as the row percentage of mitotic cells (see Fig. 1). Using the notation introduced in the previous paper the MI is

$$\mathrm{MI}(j, t) = \mathrm{SUM}_{i=1,\ldots,16} X_i/16;\ X_i = \begin{cases} 0 \text{ if } B(i, j/t) \neq 1 \\ 1 \text{ if } B(i, j/t) = 1 \end{cases}$$

where the crypt has a circumference of 16 cells.

Cluster

A cluster of mitotic cells is defined as a series of mitotic cells consecutively arranged in a vertical column (longitudinal section) or a circumferential row (transverse section), e.g. two mitotic cells, which are neighbours in a column are called a vertical pair of mitoses, those in a circumferential row are a horizontal pair, etc. Examples are shown in Fig. 1. Larger clusters of three, four, etc. adjacent mitotic cells are also possible.

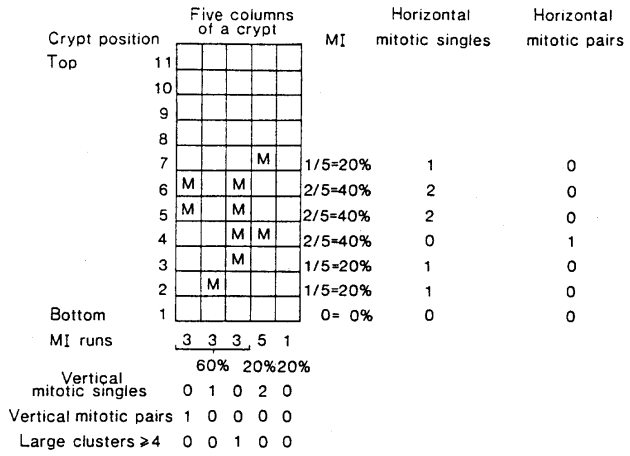

Fig. 1. Scheme of evaluation. A projection of part of the crypt epithelium is shown restricted to five adjacent crypt columns (crypt sections). Mitotic cells are indicated by M. The horizontal evaluation generates a position-dependent mitotic index (MI), the vertical evaluation can be performed according to the run concept. A run is defined as a sequence of like cells. The number of runs per column is counted. The run distribution is calculated as the relative frequency of runs of the same length (e.g. 60% of the columns have three runs). In addition, the number of singles or pairs or larger clusters of horizontally or vertically adjacent cells is counted.

MI run

In a given longitudinal crypt section (column) we also count the number of mitotic and non-mitotic sequences from the bottom to the top of the crypt, and obtain the MI run. It is defined in an analogous manner to the runs for [^{3}H]TdR-labelled cells given elsewhere (Potten *et al.*, 1982; Loeffler *et al.*, 1986). Examples are also given in Fig. 1.

VCR

The simulation of mitotic arrest after VCR is calculated as follows: when a cell enters the mitotic phase ($B(i,j/t)=1$), the progress through the cell cycle is stopped ($B(i,j/t)=B(i,j/t+1)$) and the division is suppressed. However, all other cells continue to progress through the cell cycle.

The subsequent computer calculations are usually based on 30 crypts.

Determination of T_M *and the geometrical correction factor*

In a stathmokinetic experiment with VCR the MI at a certain crypt position in longitudinal sections should increase with time according to the equation:

$$MI_S(0) = C \cdot T_M/f \qquad 0 \le t \le t_0 \qquad (1a)$$

$$MI_S(t) = C((t - t_0) + T_M)/f \qquad t_0 \le t \qquad (1b)$$

T_M is the mitotic phase duration, t the time after VCR application ($t = 0$ the start of the experiment), t_0 the time when the mitotic arrest begins to operate and f the geometrical correction factor for overestimation of mitotic figures in longitudinal crypt sections. The proportionality constant C depends on the growth fraction, cell cycle times and the cell kinetic heterogeneity. As we are unable to computer simulate the physiologic 'popping up' of dividing

cells into the lumen of the crypt, a different way of introducing the correction factor had to be found. The basic idea was that a geometrical correction factor could be replaced by a correction factor based on a time scale. Technically this can be done by defining a new mitotic phase duration

$$T_{M,sim} = T_M/f \tag{2a}$$

and a new time variable:

$$t_{sim} = (t - t_0)/f \tag{2b}$$

Equation (1) then changes to:

$$MI_{S,sim}(t_{sim}) = MI_S(0) \qquad \text{for } -t_0 \le t_{sim} < 0 \tag{3a}$$

$$MI_{S,sim}(t_{sim}) = C(t_{sim} + T_{M,sim}) \qquad \text{for } 0 \le t_{sim} \tag{3b}$$

This describes the increase of MI in model crypt columns after VCR as a linear increase with t_{sim} and an intercept at $t_{sim}=0$. Computer simulations of $MI_{S,sim}(t_{sim})$ at position 8–10 for various times t_{sim} and mitotic phase durations $T_{M,sim}$ can be compared with the experimental data before (0), and 1, 2 and 3 h after VCR. Matching the linear increase of the computer-derived $MI_{S,sim}(t_{sim})$ with the experimental $MI_S(t)$ increase leads to an estimation of f, t_0 and T_M using equations (2a) and (2b).

All subsequent model calculations (see Fig. 3 below) are performed with $t_0 = 1/2$ h, $T_{M,sim} = 1$ h and $f = 0{\cdot}66$ which were obtained as optimum values.

Statistics

A statistical test procedure was designed to prove that the leading edge of the experimental MI distribution 'MI_S' moves to higher positions. In order to make the maxima of the MI distributions from different time points comparable one has to eliminate the time factor. For this purpose we transformed the MI distributions for any time points $t \in [t_0, t_{max}]$ by multiplying each MI value with $(t_{max} - t_0 + T_M)/(t^* - t_0 + T_M)$ (see equation (1)) using t_0 and T_M as derived above (t_{max} = 3 h). The distributions obtained are split in two parts (left, position 0–12, right, position 12–21). One can then compare the left parts of the transformed distributions of the three time points with one another and similarly the right parts. For this a non-parametric U-test is used. The adequacy of the transformation is shown as it generates statistically indistinguishable left side distributions. The significance level of 5% in a two-sided test is used.

RESULTS

MI distribution after VCR

Mitotic accumulation data after VCR were examined. They are shown all together in Fig. 2 and clearly show the mitotic accumulation as an increase of the maximum and a migration of mitotic cells to higher crypt positions. This shift to higher positions is statistically significant if one compares the control or 1 h VCR MI distribution with the 3 h VCR distribution. The movement of the leading edge amounts to two to four cell positions (see Fig. 2).

Mitotic phase duration, geometrical correction factor and onset of mitotic arrest

Using the MI distributions it is possible to deduce the mitotic phase duration T_M, the time of onset of mitotic arrest t_0 and the geometrical correction factor f for mitotic overestimation from VCR experiments. For this purpose model simulations of MI distributions are performed (see below). Matching the computer MI distributions to the experimental MI distributions one finds

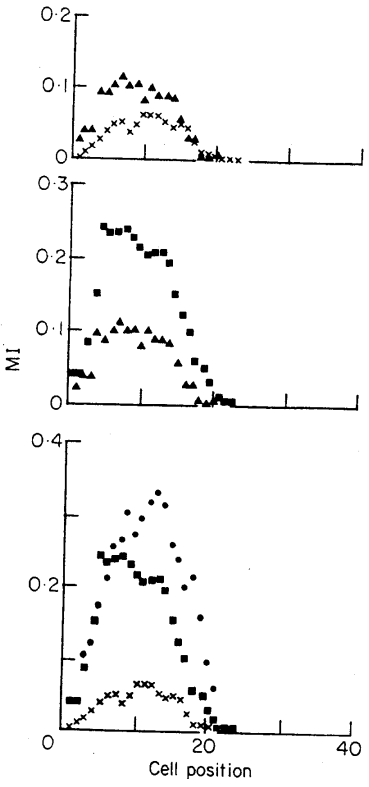

Fig. 2. Mitotic accumulation data. Mitotic index related to crypt position: (×) Control; (▲) 1, (■) 2, (●) 3 h after mitotic block with 0·02 mg/mouse of vincristine. Note the increase of the distribution with time and the movement of the right edge by about two to four cell positions towards the villus. This movement is statistically significant.

a factor f of about 0·66, a T_M of about 0·66 h and a t_0 of 0·5 h. The accuracy of our determination is of the order of $\pm 20\%$.

Simulations with a shorter mitotic phase duration of the late transit cells (e.g. $T_M = 0.33$ h) produced MI_S too low at the top of the crypt. Likewise, a longer mitotic phase duration at the bottom of the crypt produced too high MI values compared with the data. Therefore, we conclude that T_M is almost the same for all crypt cells independent of cell position. Likewise, positional variation of the geometrical correction factor f was not concluded.

Modelling MI distributions

Once the correction factor and the mitotic phase duration are known it is possible to relate complete experimental MI distributions obtained from crypt sections to computer-derived MI curves where the higher chance of sectioning mitoses does not play a role. Position-dependent MI distributions for models E, F and H were calculated and compared with the data. The results are shown in Fig.3 (top row). The data are shown as measured, the model curves are obtained by simulating the overscoring of mitoses in the data due to geometrical rearrangement by an appropriate elongation of the time scale (see equation (3)). The MI curves of all three models fit the experimental data well. There is only a slight overestimate at the right-hand side of the distribution.

Model MI curves after 1, 2 and 3 h of mitotic arrest were calculated and compared with the data (Fig. 2 second–fourth row). Again the raw data (uncorrected) are compared with the

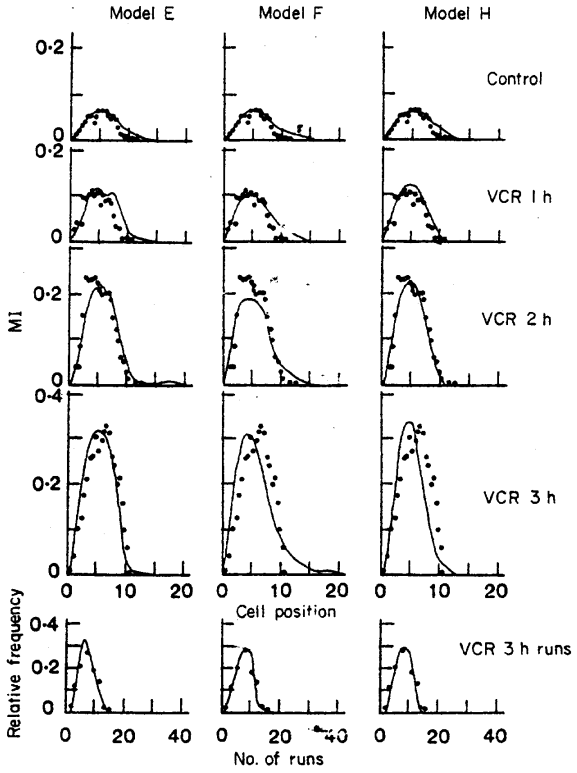

Fig. 3. Comparison of mitotic accumulation data with model scenarios. The data from Fig. 2 have been redrawn to compare them with three computer scenarios. Left column, model E (local age-dependent displacement with three neighbours); middle column, model F (local age-dependent displacement with five neighbours); right column, model H (random displacement with transit cell cut-off; see Loeffler *et al.* (1986) for further details). Row 1, position-dependent mitotic index (MI), no vincristine (VCR), control; rows 2–4, MI 1, 2 and 3 h after VCR; row 5, MI run 3 h after VCR. The model calculations are corrected for geometrical considerations to make them comparable with data. The increase of the MI after VCR is reproduced well by all models. A movement of the mitotic distribution in the absence of cell division is not seen in the model curves as is to be expected from the way they are generated. This discrepancy supports a new concept of cell migration and its interaction with the crypt shape. In the absence of mitotic activity the crypt will shrink and adjacent cell columns will merge such that the output of cells to the villus will remain unchanged at least for a short time.

corrected model data. All three models produced MI distributions which increased with time. Models E and H showed comparably good fits to the experimental data, while model F produced pronounced tails in the distributions. Here the mechanisms generating age ordering (younger cells positioned below older cells) are not sufficient. Some transit cells appear at positions where only post-mitotic cells should be found.

Table 1. Results of the cluster analysis

		Mitotic clusters					
			Without VCR		3 h VCR†		
	Lateral displacement (%)	MI (%)	Vertical clusters/ crypt	Horizontal clusters/ crypt	Vertical clusters/ crypt	Large vertical clusters/ crypt‡	Horizontal clusters/ crypt
Experiment§	Unknown	3·3	0·24	ND	11·1	0·8	ND
Model A*¶ (vertical displacement)	0	4·5	1·4 ± 0·3	0·5 ± 0·15	15·5 ± 1·0	4·5 ± 0·6	12·3 ± 1·3
Model E¶ (local age-dependent displacement with three neighbours)	42	3·6	1·7 ± 0·3	0·8 ± 0·3	17·5 ± 0·7	3·5 ± 0·5	13·9 ± 1·1
Model F¶ (local age-dependent displacement with five neighbours)	80	4·4	0·7 ± 0·3	1·1 ± 0·4	15·7 ± 1·1	2·8 ± 0·4	14·2 ± 1·4
Model H¶ (random displacement with cut-off at position 12)	63	3·9	0·5 ± 0·15	0·3 ± 0·2	12·7 ± 0·9	1·5 ± 0·4	10·6 ± 1·0

Average ± SEM.
* Rejected, because of bad labelling index run fits (Loeffler *et al.*, 1986).
† t_{sim} = 3·75 h.
‡ Large clusters have a size of 4 or larger.
§ Data obtained from 200 half crypt sections.
¶ Calculations based on 10 model crypts (equivalent to 160 half crypt sections).
VCR, Vincristine; MI, mitotic index; ND, not done.

It is important to note that the right-hand tail of the experimental curves moves slightly to higher positions with time (Fig. 2). However, all model curves remain stationary and only increase in height. As in all models cell movement only occurs as a consequence of cell division, the failure of the model is not surprising and the discrepancy between the model and the data provides evidence for the migration of mitotic cells in the absence of mitosis.

MI run

Figure 3 (fifth row) shows MI runs after 3 h VCR both in the model crypts and in the data. The run distributions for all models fit the data in a satisfactory manner. Discrepancies, however, appear in the more detailed cluster analysis.

Vertical clusters

Without VCR

The frequency of clusters of mitotic cells in the data of longitudinal crypt sections was evaluated and compared with model evaluations. The results are shown in Table 1 together with the MI and the percentage of lateral displacement in the various models after mitosis. The frequency of clusters generated by all models is higher than actually found in the data, with model H being the closest to the data.

3 h after VCR

Table 1 also shows the clusters of mitotic cells after 3 h VCR in the experimental data and in model crypts. The percentage of clusters and in particular the percentage of long vertical clusters (clusters with 4 or more cells) was found to be much higher in all models than in the data. This was particularly the case in model A. Since no lateral migration takes place in this model, the cell kinetic synchrony of daughter cells leads to the fact that many neighbouring cells in a column enter mitosis at nearly the same time. Similarly, in model E the number of long clusters was too high, suggesting that 42% lateral displacement is insufficient. For models F and H the discrepancy is less dramatic but still present.

Horizontal clusters

Table 1 shows the clusters predicted by the various models for transverse sections of the crypt before and after VCR. Comparable experimental data are not available at present. The models, however, predict different results that may be experimentally testable especially to distinguish model H from the others.

Relationship between LI and MI

Without VCR the LI distributions always reach higher cell positions than the MI distributions. This is true for the data as well as for the model calculations. After 3 h of VCR this pattern changes. The experimental MI tail appears at higher cell positions than the experimental LI evaluated before application of VCR. Apparently the cells migrated in the absence of mitosis by two to four positions in 3 h, a feature that none of the models could generate at present.

DISCUSSION

In this analysis we suggest a new method to derive from MI arrest data simultaneously three relevant parameters: the geometrical correction factor f for overestimating mitotic cells, the time t_0 of the onset of mitotic arrest and the M phase duration T_M. The method is based on a comparison of data with a recently developed simulation model of crypt proliferation (Loeffler *et al.*, 1986).

In order to make the experimental and theoretical MI distributions for longitudinal crypt sections comparable a geometrical correction factor 'f' had to be determined. This factor f corrects for the fact that mitotic figures tend to be placed closer to the lumen of the crypt so that they have a higher chance of being sectioned and appearing with a column of cells to which they do not belong. Sectioning of cylindrical crypts therefore leads to an overestimation of the number of mitoses and therefore of the MI compared with a theoretical measurement in a crypt that is rolled out and then sectioned (as with the model $MI_{S,sim}$). We have introduced a new way to estimate this correction factor by matching the time scales of the MI increase in the model and the data in VCR accumulation experiments. This correction factor f is an actual phenomenological factor determined by comparing a model where no correction is involved with actual section data where MI are overestimated. A correction factor of 0·66 is obtained by this new procedure which seems to be nearly the same for all crypt positions.

Another direct attempt to estimate this correction factor was suggested earlier by Tannock (1967). This factor called f_T takes direct determination of the position of mitotic cells into account. It partially corrects the experimental situation but we believe is an oversimplification since the size of the mitotic figures and the peripheral nuclei are not the same as was assumed by Tannock. Furthermore, the thickness of the section and its orientation (transverse or longitudinal) influences the measurements (Potten *et al.*, 1988). In our hands the determination

of f_T taking these aspects into account yields a value of 0·56 in 1 μm sections and 0·53 in 3 μm sections in murine ileum. However the method still has some ambiguities as is discussed in the accompanying paper (Potten *et al.*, 1988). Therefore, we have looked for an alternative experimental determination of the correction factor counting the number of mitotic figures and cells seen in whole crypts as well as in sections. One thereby derives a factor f_D of 0·59 (Potten *et al.*, 1988). For reasons discussed in the accompanying paper the value of f_D is suspected to be more precise than that obtained by the method Tannock used. Although quite different in the way of determination this value for f_D is close to the 0·66 value derived by the independent model exercise.

A method to determine T_M from MI arrest data has been suggested by Al-Dewachi *et al.* (1975) under the assumption that the time to onset of VCR action is known. They assume t_0 to be 20 min which is within the confidence limits of the 30 min value estimated by our procedure (15–45 min). If we use Al-Dewachi's procedure to determine T_M we obtain an estimate which is consistent with the value derived from the model evaluation. The latter method is somewhat more accurate in our case because it exploits data from many cell positions simultaneously and can therefore be applied if the time points of measurement are less frequent than required for Al-Dewachi's regression analysis. The models used for the analysis were first introduced to describe LI and labelled clustering experiments (Loeffler *et al.*, 1986). Now we show that specification of three parameters f, T_M and t_0 enables a good fit also to the steady state MI and mitotic arrest data. The models also simulate the MI run data very well as a measure of the overall clustering picture (Fig. 2, bottom) but consistently overestimate the number of vertical mitotic clusters that have more than four mitotic figures in a row.

In conjunction with the previous paper the interpretation is strengthened that most kinetic data in the steady state crypt can be explained with our model, although some of the assumptions may be oversimplifications of the real situation. The crypt may not be cylindrical, circadian variations may complicate the situation, the reaction of the cells to VCR may be described too simply and the geometrical correction factor may depend on the time after VCR. The most important oversimplification, however, we believe is the use of a rigid cell matrix and the strict coupling of cell migration to mitosis. Lateral or vertical cell displacement without cell division could only occur if either 'holes' are left in the matrix or if at least some cells move downwards. As both are excluded in the model it is unable to produce cell migration without mitotic activity. Therefore, the right-hand tail of the model MI curve does not move when mitotic arrest is simulated in contrast with the MI data. In addition, the model produced too many long vertical clusters after 3 h of VCR compared with the data. Both discrepancies may, however, be explained. As no migration takes place in the model long clusters of mitotic cells will develop since many adjacent cells originate from the same mother or grandmother cell and enter mitosis fairly simultaneously thereby generating clusters. As this is not found experimentally we have to conclude that lateral displacement occurs even in the absence of mitosis. Non-mitotic cells from adjacent columns might move laterally thereby breaking up clusters of mitoses and moving the cells in these columns one position upwards. The merging of adjacent cell columns could therefore in principle explain the major discrepancies between the data and the model mentioned. But how could this effect of merging columns be generated? From the previous LI and run simulations and from the present results two main features about cell movement in the crypt are noteworthy: (1) The probability of lateral displacement after mitosis must be high to explain the LI run data. This migration produces disorder in the sense that older cells may be arranged on the same level as young cells. On the other hand, there has to be an ordering mechanism independent of mitotic activity which tends to restore the observed order (equal age in similar positions) and thereby explain the sharp transition from mitotic to postmitotic

cells indicated by the LI. (2) When mitosis is stopped migration continues. This also happens after irradiation. Although a mitotic arrest is observed immediately after irradiation (Chwalinski & Potten, 1986) the crypt cells continue their vertical migration for a short time since the leading edge of the LI distributions still moves towards the villus (Potten *et al.*, 1983; Kaur & Potten, 1986). Because of this cell loss in the absence of mitosis the crypt shrinks in circumference (Potten & Loeffler, 1987).

These points can be uniformly explained by the following hypothesis. In the steady state there exists a dynamic balance between external forces (e.g. elastic elements) tending to contract the circumference of the crypt and an internal pressure resulting from the lateral cell displacement connected to mitotic activity. The frequent lateral positioning of daughter cells would thus stabilize the circumference. If mitotic activity ceases the contracting forces become overwhelming and lead to a merging of columns thereby breaking up long clusters of mitotic or labelled cells. This merging process would, however, be connected to vertical displacement (which still goes on) which explains the movement of the MI distribution after VCR. In this concept lateral and vertical displacement could be two independent processes. While the lateral mitotic displacement produces the disorder, the vertical migration has to restore the age ordering by a local age-dependent displacement or by a cut-off situation. The idea may help explain the overall flask shape of the crypt. Where mitotic activity is low or absent the crypt would taper as it does at both the base and the top.

Having this interpretation in mind the differences between models E,F and H presented in Table 1 should not be used to select one over the other because the merging of adjacent columns resulting in the breaking up of large clusters and the change in the crypt geometry cannot at the moment be simulated.

Corresponding models with a dynamic crypt geometry will, however, be worked out in the future. They should in particular be able to simulate crypts after cytotoxic perturbations where changes of the crypt shape play a large role.

It may finally be important to note that the lateral displacement of newborn cells may not necessarily be correlated to the so-called 'mitotic axis' of bipolar mitotic figures (anaphases). It was recently reported that the majority of anaphase figures (2/3) is orientated in a vertical direction (Potten *et al.*, 1988). Once the two cells have been formed, their final positioning may, however, be determined by different mechanisms. To facilitate this repositioning the mitotic figures in the crypt may leave the basal cell layer to position themselves closer to the lumen of the crypt. Like 'balloons' the new cells may want to look for new 'landing positions' which may then be lateral in most cases. Therefore, it seems doubtful whether data on mitotic axes in the crypt have any relevance with respect to cell positioning. This may be different in other tissues.

In summary the present model analysis of mitotic data from the steady state crypt generated a new estimate for T_M taking the geometrical correction factor for MI into account. The MI increase after VCR can quantitatively be understood and the previous hypothesis of a fairly large percentage of lateral cell displacements was further supported and extended. The inability of the model to reproduce the cluster data and the vertical cell migration in the absence of mitotic activity suggests that adjacent cell columns can merge. This indicates that the normal crypt geometry may be in dynamic equilibrium between lateral merging and mitotic expansion (see also Potten & Loeffler, 1987).

ACKNOWLEDGMENTS

We would like to thank Paula Jones and Caroline Chadwick for their technical help. This work has been supported by the Cancer Research Campaign (UK) and the Minister of Science of North-Rhine-Westfalia (F.R.G.).

REFERENCES

AL-DEWACHI, H.S., WRIGHT, N.A., APPLETON, D.R. & WATSON, A.J. (1975) Cell population kinetics in the mouse jejunal crypt. *Virchows Arch. B. Cell Pathol.* **18**, 225.

CHWALINSKI, S. & POTTEN, C.S. (1986) Radiation induced mitotic delay duration, dose and cell position dependence in the crypts of the small intestine in the mouse. *Int. J. Radiat. Biol.* **49**, 809.

KAUR, P. & POTTEN, C.S. (1986) Cell migration velocities in crypt after cytotoxic insult are not dependent on mitotic activity. *Cell Tissue Kinet.* **19**, 601.

LOEFFLER, M., STEIN, R., WICHMANN, H.E., POTTEN, C.S., KAUR, P. & CHWALINSKI, P. (1986) Intestinal cell proliferation. I. A comprehensive model of steady state proliferation in the crypt. *Cell. Tissue Kinet.* **19**, 627.

MEINZER, H.P. & SANDBLAD, B. (1985) A simulation model for studies of intestine cell dynamics. *Comp. Prog. Biomed.* **21**, 85.

POTTEN, C.S. & HENDRY, J.H. (1985) The microcolony assay in mouse small intestine. In *Cell Clones: Manual of Mammalian Cell Techniques* (Ed. by Potten, C.S. & Hendry, J.H.), p.50. Churchill Livingstone, Edinburgh.

POTTEN, C.S. & LOEFFLER, M. (1987) A comprehensive model of the crypts of the small intestine of the mouse provides insight into the mechanisms of cell migration and the proliferation hierarchy. *J. Theor. Biol.* **127**, 381.

POTTEN, C.S., CHWALINSKI, S., SWINDELL, R. & PALMER, M. (1982) The spatial organization of the hierarchical proliferative cells of the crypt of the small intestine into clusters of 'synchronized' cells. *Cell Tissue Kinet.* **15**, 351.

POTTEN, C.S., HENDRY, J.H., MOORE, J.V. & CHWALINSKI, S. (1983) Cytotoxic effects in gastro-intestinal epithelium (as exemplified by small intestine). In *Cytotoxic Insult to Tissue* (Ed. by Potten, C.S. & Hendry, J.H.), p.105. Churchill Livingstone, Edinburgh.

POTTEN, C.S., ROBERTS, S.A., CHWALINSKI, S., LOEFFLER, M. & PAULUS, U. (1988) Scoring mitotic activity in longitudinal sections of crypts of the small intestine. *Cell Tissue Kinet.* **21**, 231.

TANNOCK, I.F. (1967) A comparison of the relative efficiencies of various metaphase arrest agents. *Exp. Cell. Res.* **47**, 345.

WRIGHT, N. & ALISON, M. (1984) *The Biology of Epithelial Cell Populations*, Vol. 2. Clarendon Press, Oxford.